

# End-to-end Driving in High-Interaction Traffic Scenarios with Reinforcement Learning

Yueyuan Li, Mingyang Jiang, Songan Zhang, Wei Yuan, Chunxiang Wang, and Ming Yang

**Abstract**—Dynamic and interactive traffic scenarios pose significant challenges for autonomous driving systems. Reinforcement learning (RL) offers a promising approach by enabling the exploration of driving policies beyond the constraints of pre-collected datasets and predefined conditions, particularly in complex environments. However, a critical challenge lies in effectively extracting spatial and temporal features from sequences of high-dimensional, multi-modal observations while minimizing the accumulation of errors over time. Additionally, efficiently guiding large-scale RL models to converge on optimal driving policies without frequent failures during the training process remains tricky. We propose an end-to-end model-based RL algorithm named Ramble to address these issues. Ramble processes multi-view RGB images and LiDAR point clouds into low-dimensional latent features to capture the context of traffic scenarios at each time step. A transformer-based architecture is then employed to model temporal dependencies and predict future states. By learning a dynamics model of the environment, Ramble can foresee upcoming traffic events and make more informed, strategic decisions. Our implementation demonstrates that prior experience in feature extraction and decision-making plays a pivotal role in accelerating the convergence of RL models toward optimal driving policies. Ramble achieves state-of-the-art performance regarding route completion rate and driving score on the CARLA Leaderboard 2.0, showcasing its effectiveness in managing complex and dynamic traffic situations.

**Index Terms**—Deep reinforcement learning, driving decision-making, end-to-end driving.

## I. INTRODUCTION

In real-world traffic scenarios, drivers must continuously interact with other vehicles and road users, negotiating situations such as merging, turning, overtaking, and reacting swiftly to traffic signals and lane markings. The ability to understand and respond to these dynamic and interactive situations is essential for autonomous driving. However, traditional rule-based policymakers struggle to generalize across the various traffic events. Moreover, simply relying on limited human driving data through Imitation Learning (IL) proves inadequate in addressing the diverse and unpredictable nature of driving. As evidence, CARLA presents 38 highly dynamic and

interactive scenarios in its Challenge 2023. Despite advances in the field, no solution has been able to fully master these tasks without privileged information, with the best-performing implementations achieving only 18% route completion rate, highlighting the need for more robust driving solutions [1].

Reinforcement Learning (RL) has shown significant potential in addressing complex traffic scenarios. Unlike IL, which is confined to replicating human behavior based on predefined datasets, RL may explore novel and efficient driving policies through continuous environmental interaction. With the guidance of reward signals, a well-designed RL framework can optimize its behavior towards different driving purposes, such as safety, efficiency, or passenger comfort. The RL algorithm has outperformed human champions in the F1 racing competition [2]. Additionally, in the CARLA simulator, RL-based models have achieved the highest route completion rates and driving scores in Leaderboard 1.0 and 2.0 as long as privileged information is available [3, 4]. These successes suggest the promise of RL as a robust approach to tackling the challenges inherent in dynamic traffic scenarios.

One of the primary challenges in applying RL to realistic driving scenarios is effectively representing the high-dimensional observation space. Most well-known RL algorithms, such as DQN, SAC, PPO, and the Dreamer family, are designed to handle low-dimensional state spaces and only have their performance tested in naive environments like Atari and Mujoco [5, 6]. However, realistic driving scenarios involve complex sensory inputs, such as high-resolution camera images, LiDAR point clouds, and radar signals, that require more sophisticated feature extraction and representation methods [7]. Bridging this gap between high-dimensional sensory input and RL algorithms remains a critical obstacle in translating its successes from toy cases to real-world applications.

Another obstacle lies in effectively leveraging the temporal features inherent in traffic scenarios. Most RL methods rely on the Markov assumption, which presumes that the current state contains all necessary information for decision-making. However, in autonomous driving, understanding the intentions and behaviors of other traffic participants requires capturing temporal dependencies that extend beyond the current state. Integrating this temporal information is crucial for making informed decisions in dynamic environments [8].

This paper proposes an end-to-end model-based RL algorithm called Ramble to address these challenges. Ramble is designed to process multi-modal, high-dimensional sensory inputs while effectively managing the temporal complexities of interactive traffic environments. By learning a dynamics model of the environment, Ramble can predict future outcomes

This work is supported by the National Natural Science Foundation of China (62173228). Ming Yang is the corresponding author.

Yueyuan Li, Mingyang Jiang, Chunxiang Wang, and Ming Yang are with the Department of Automation, Shanghai Jiao Tong University, Key Laboratory of System Control and Information Processing, Ministry of Education of China, Shanghai, 200240, CN (phone: +86-21-34204533; email: [MingYANG@sjtu.edu.cn](mailto:MingYANG@sjtu.edu.cn)).

Songan Zhang is with the Global Institute of Future Technology, Shanghai Jiao Tong University, Shanghai, 200240, CN.

Wei Yuan is with the Innovation Center of Intelligent Connected Vehicles, Global Institute of Future Technology, Shanghai Jiao Tong University, Shanghai, 200240, CN.

and plan actions accordingly, leading to more informed and strategic decision-making.

Through our implementation, we observed that prior experience in feature extraction and decision-making plays a vital role in guiding large-scale RL models toward convergence to a reasonable policy. To this end, we propose a method to inject privileged information into the RL framework, which can effectively resolve the cold-start training issue. The contributions of this paper are as follows:

- 1) We design the first RL-based driving model to accomplish routes in CARLA Leaderboard 1.0 and 2.0 without relying on privileged information at the inference phase.
- 2) We propose a method to injects privileged information and prior driving experience into an RL framework, which can effectively resolve the cold-start training issue.
- 3) We establish a reproducible baseline for the CARLA Leaderboard 2.0 by migrating multiple state-of-the-art algorithms from the CARLA Leaderboard 1.0, providing the research community with a solid foundation for future advancements.

## II. RELATED WORKS

### A. End-to-end Driving with Deep Learning

End-to-end driving models map raw sensor inputs directly to driving actions. This framework aims to avoid explicit feature extraction, which may result in the omission of crucial latent features and the accumulation of errors. Most of the end-to-end driving models fall into two main classes: IL and RL [9].

In recent years, IL-based driving models have become the mainstream in the field. They primarily focus on leveraging features from high-dimensional inputs and imitate expert behavior during policy learning for rapid convergence. This approach has been popular since the introduction of the first end-to-end driving model, DAVE-2 [10]. Many IL-based driving models have since devoted to improving perception capabilities. Notable examples include Transfuser and InterFuser, which utilize transformer-based architectures to integrate features from multi-view images and LiDAR point clouds [11, 12]. Models such as ReasonNet and CarLLaVA further refine performance by generating intermediate features with semantic meaning, improving context awareness [1, 13]. Besides, some research attempts to ensemble outputs. For instance, TCP combines action commands with waypoint predictions, which is an effective improvement adopted by many subsequent works [14]. Similarly, Transfuser++ enhances performance by decoupling waypoint prediction from velocity estimation [15]. However, the main drawback of IL-based driving models is their reliance on high-quality trajectory data or command records from experts [16–18], so their performance naturally degrade in corner cases or unseen scenarios. Furthermore, due to their limited exploration ability, these models struggle in traffic scenarios with dense interaction, a limitation clearly highlighted in CARLA Leaderboard 2.0.

While IL-based methods have thrived, RL-based driving models have encountered more challenges. Despite early efforts in specific scenarios [19–21], researchers have found that training RL agents is costly due to the need for real-time

feedback from the environment. Additionally, model-free RL-based driving models face significant challenges in processing high-dimensional inputs and achieving stable convergence to a reasonable policy [22, 23]. While models like Roach and Think2Drive have demonstrated the potential of RL in driving decision-making, their reliance on privileged information makes them impractical for real-world applications [3, 4]. To enable models to learn scenario context from complex raw sensor data, Peng *et al.* proposed using expert driving behavior to guide the learning process, which has been shown to converge to safer policies [24]. RL-based driving models are expected to achieve better generalization performance than IL-based models. While RL-based models are expected to generalize better due to their ability to explore the environment, they still lag behind IL-based models in overall performance.

### B. Model-based Reinforcement Learning

RL is a potential learning paradigm for exploring behavioral strategies in complex environments. Model-based RL distinguishes itself by learning a dynamics model of the environment, which enables it to plan actions with foresight into future outcomes [25]. This approach tends to be more sample-efficient and capable of handling more complex tasks compared to model-free RL.

Model-based RL has achieved impressive performance on well-known benchmarks like Atari. Many successful model-based algorithms are built upon the foundational ideas of the world model framework [26], which emphasizes learning compact representations of the environment to predict future states and guide planning. SimPLe employs a basic neural network to model environment dynamics and incorporates a stochastic model to handle the environment uncertainty, resulting in higher sample efficiency than model-free methods [27]. In PlaNet, Hafner *et al.* introduced the recurrent state-space model to better manage environments with complex variations, providing higher cross-domain robustness [28]. This innovation set the stage for the widely adopted Dreamer family of algorithms [6]. Beyond advancements in underlying mechanisms, researchers are continuously upgrading the network architectures within model-based RL frameworks. For instance, IRIS demonstrates the effectiveness of transformer-based models in learning environment dynamics [29], while STORM enhances performance further by integrating a stochastic model to better address environmental uncertainty [30].

Despite the success of model-based RL in toy environments, its application in real-world scenarios remains challenges. Very few attempts have been made to apply model-based RL to autonomous driving [4]. The main obstacle is the difficulty of learning an accurate dynamics model from high-dimensional sensor inputs. The complexity of the traffic scenarios makes it challenging to predict future states. In this paper, we will show that Ramble is a promising model-based RL algorithm to tackle the issues mentioned above and is applicable to autonomous driving.

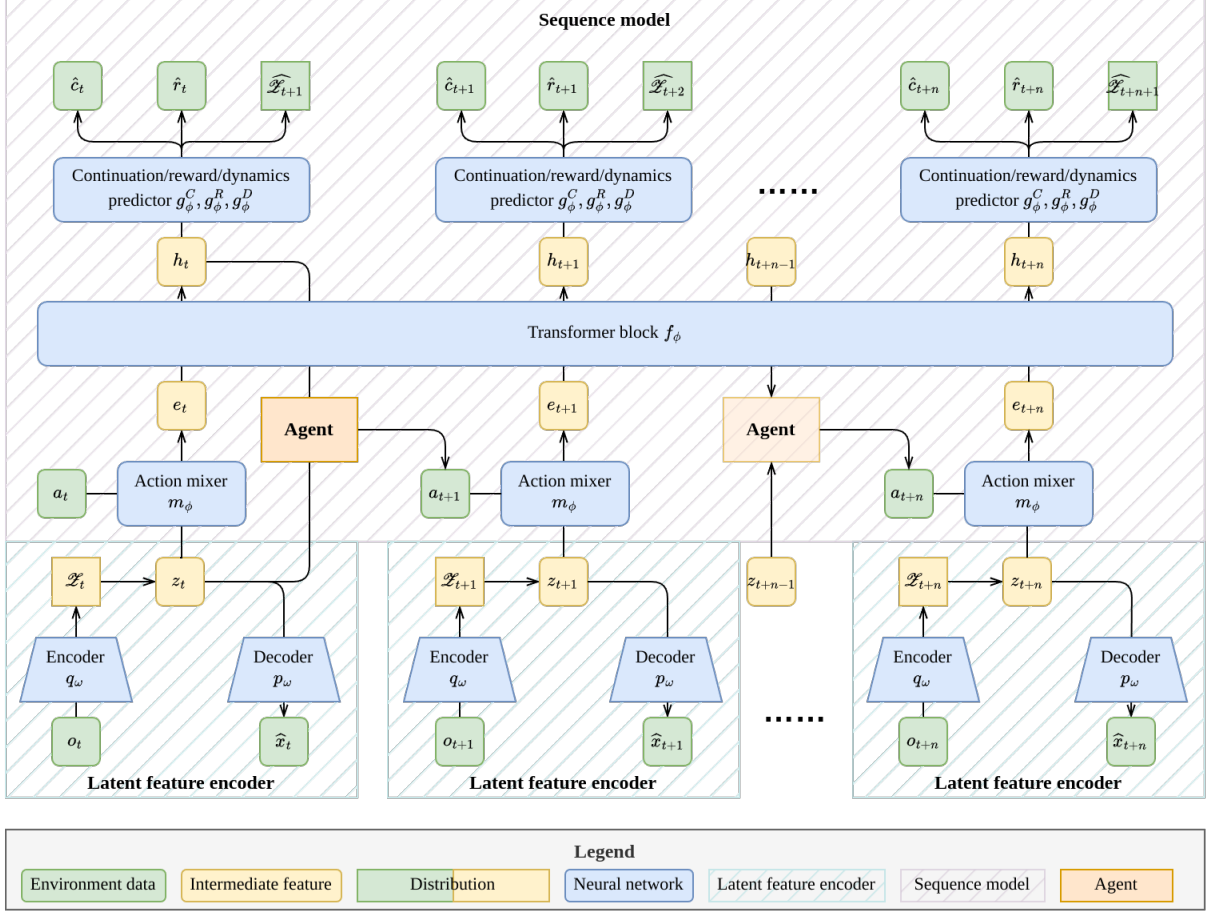


Fig. 1. The overview of Ramble at training phase.

### III. METHOD

#### A. Overview

The overall structure of Ramble is illustrated in Figure 1. Our approach builds upon the framework established in the original world model [26]. Following this paradigm, Ramble first processes high-dimensional input observations, encoding them into abstract, compressed latent features. These latent features are then fed into a sequence model, which captures the temporal information across a series of observations. The latent features obtained directly from the observations and those containing temporal information are then integrated as inputs to the agent, which makes driving decisions.

#### B. Latent Feature Encoder

The feasibility of model-based RL agents has been proven in Atari games, where observations consist of relatively simple  $210 \times 160$  pixel images [31]. However, in the context of autonomous driving, the observation space is typically much higher in dimension. Lower-dimensional input would not provide sufficient information for the agent to make decisions. Consequently, it is necessary to design a more powerful encoder capable of compressing high-dimensional input observations into a lower-dimensional latent space.

Our input observations consist of multi-view RGB images and LiDAR point clouds. Detailed sensor configurations are provided in Appendix B. The RGB images are captured at a resolution of  $640 \times 480$  from the front, left, right, and rear views. The LiDAR data comprises approximately 31,000 points from a  $360^\circ$  scan. These inputs are recorded at 10 Hz.

To effectively manage the complex input data, we designed a latent feature encoder inspired by BEVFusion [32]. The structure of this encoder is shown in Figure 2. Raw camera data is initially processed by a Swin Transformer [33] to extract multi-scale features, which are then merged into a feature map using an FPN [34]. Following the core concept of BEVFusion, the camera features are projected into BEV and mapped onto 3D grids. Simultaneously, LiDAR point clouds are voxelized and mapped to 3D grids using a PointPillars network [35]. Since the point cloud features are natively in BEV format, no additional view transformation is needed. The image and point cloud features are then concatenated and fused through a convolutional neural network. Finally, the route points information is processed by a multi-layer perceptron and fused with the sensory data by cross-attention mechanism and sent to the Variational Autoencoder (VAE).

The feature extraction network and the VAE’s encoder together are referred to as the observation encoder  $q_\phi(\omega)$ ,

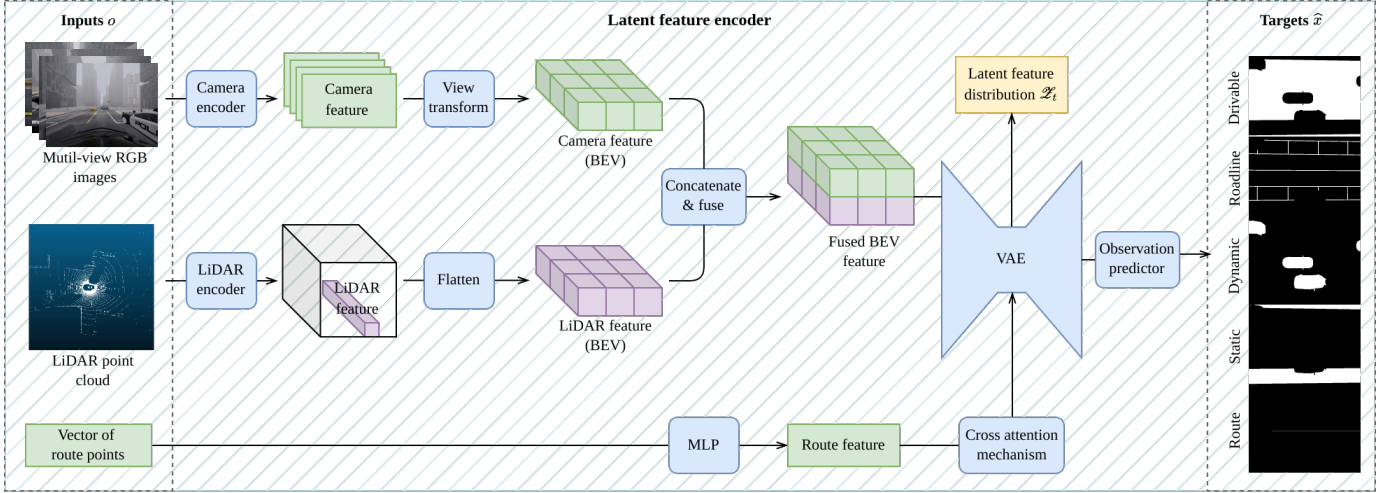


Fig. 2. The structure of latent feature encoder.

while the VAE’s decoder is denoted as the observation decoder  $p_\phi(\omega)$ .  $\omega$  represents the parameters of the latent encoder’s network. To enhance the generalization ability of the whole model, the latent encoder does not directly output the latent feature  $z_t$ . Instead, it models the environment dynamics with a distribution  $\mathcal{Z}_t$ , from which the latent feature is sampled [36].

$$\text{Observation encoder:} \quad z_t \sim \mathcal{Z}_t = q_\omega(z_t|o_t)$$

$$\text{Observation decoder:} \quad \hat{x}_t = p_\omega(z_t)$$

here  $o_t$  represents the raw sensor observations at time  $t$ , and  $\hat{x}_t$  is the reconstructed observation.

We use two different letters because the encoder’s output is not the same as the input in our model. The raw sensor observation is too complex for a reconstruction task. Moreover, the encoder is heavy in parameters, so it is irrational to expect it to learn the necessary latent features by training directly alongside the rest of Ramble. To address this, we pre-train the encoder with BEV binary semantic segmentation  $x_t$  as the label. This approach helps discover features that may be critical for driving tasks. A detailed explanation of the training process can be found in Section III-E. Given the imbalance in the semantic labels, we use sigmoid focal loss to handle the reconstruction loss [37]. The component loss functions used during the pre-training phase are defined as follows:

$$\begin{aligned} \mathcal{P}_t &= x_t \cdot \sigma(\hat{x}_t) + (1 - x_t) \cdot (1 - \sigma(\hat{x}_t)) \\ \mathcal{L}_t^{\text{rec}}(\omega) &= -\alpha(1 - \mathcal{P}_t)^\gamma \cdot \log(\mathcal{P}_t) \\ \mathcal{L}_t^{\text{kl}}(\omega) &= \text{KL}(q_\omega(z_t|o_t)||p_\omega(z_t)) \end{aligned}$$

where  $\sigma(\cdot)$  means the sigmoid function.  $\mathcal{P}_t$  is the probability of the reconstructed observation being correct.  $\mathcal{L}_t^{\text{rec}}(\omega)$  is the reconstruction loss, whose sample balancing factor is  $\alpha$  and focusing parameter is  $\gamma$ .  $\mathcal{L}_t^{\text{kl}}(\omega)$  is the KL divergence loss.

Gathering them together, we can obtain the loss function  $\mathcal{L}(\omega)$  for pre-training the latent feature encoder:

$$\mathcal{L}_t(\omega) = \mathcal{L}_t^{\text{rec}}(\omega) + \beta^{\text{kl}} \mathcal{L}_t^{\text{kl}}(\omega)$$

where  $\beta^{\text{kl}}$  as a scalar factor that balances the reconstruction and KL divergence losses.

### C. Sequence Model

To extract temporal information from the sequence of latent features, it is necessary to apply capable of capturing inter-connections. The initial version of the world model uses a Long Short-Term Memory (LSTM) network [26]. However, the Transformer architecture has been proven to be more effective at capturing long-range dependencies in sequential data [36]. Therefore, we follow the design of STORM to implement the sequence model with a transformer [30]. As is demonstrated in the following equations, the latent feature  $z_t$  sampled from  $\mathcal{Z}_t$  is combined with the action  $a_t$ , using multi-layer perceptron (MLP) and concatenation. This manipulation is denoted as  $m_\phi$ , and the mixed feature is  $e_t$ . We then adopt a GPT-like transformer  $f_\phi$  with a stochastic attention mechanism to process the mixed feature. The output of the transformer is the hidden state  $h_t$ . Finally, the hidden state is fed into three different MLPs:  $g_\phi^D$  predicts the next environment dynamics distribution,  $g_\phi^R$  predicts the reward, and  $g_\phi^C$  predicts the continuation probability.  $\phi$  represents the parameters of the sequence model. The expressions of these components are as follows:

$$\begin{aligned} \text{Action mixer:} & \quad e_t = m_\phi(z_t, a_t) \\ \text{Sequence model:} & \quad h_{1:T} = f_\phi(e_{1:T}) \\ \text{Dynamics predictor:} & \quad \hat{\mathcal{Z}}_{t+1} = g_\phi^D(\hat{z}_{t+1}|h_t) \\ \text{Reward predictor:} & \quad \hat{r}_t = g_\phi^R(h_t) \\ \text{Continuation predictor:} & \quad \hat{c}_t = g_\phi^C(h_t) \end{aligned}$$

The sequence model is trained jointly with the latent feature encoder, and its loss function comprises multiple components, each targeting a different optimization goal. The dynamics loss,  $\mathcal{L}_t^{\text{dyn}}$ , and the representation loss,  $\mathcal{L}^{\text{rep}}$ , guide the prediction of the next distribution and maintain similarity between the sequence model’s output and the encoder’s latent features. The reward prediction error is captured by  $\mathcal{L}_t^{\text{rew}}$  using symlog two-hot loss, while the continuation prediction error



is represented by  $\mathcal{L}_t^{\text{con}}$  using binary cross-entropy loss.

$$\begin{aligned}\mathcal{L}_t^{\text{dyn}}(\phi) &= \max(1, \text{KL}[\text{sg}(q_\phi(z_{t+1}|o_{t+1}))\|g_\phi^D(\hat{z}_{t+1}|h_t)]) \\ \mathcal{L}_t^{\text{rep}}(\phi) &= \max(1, \text{KL}[q_\phi(z_{t+1}|o_{t+1})\|\text{sg}(g_\phi^D(\hat{z}_{t+1}|h_t))]) \\ \mathcal{L}_t^{\text{rew}}(\phi) &= \text{symlog}(\hat{r}_t, r_t) \\ \mathcal{L}_t^{\text{con}}(\phi) &= c_t \log \hat{c}_t + (1 - c_t) \log(1 - \hat{c}_t)\end{aligned}$$

Here,  $\text{sg}(\cdot)$  is the stop-gradient function, and  $\text{symlog}(\cdot)$  is the symlog two-hot loss.

The total loss  $\mathcal{L}_t$  is a weighted sum of these components:

$$\mathcal{L}_t(\phi) = \mathbb{E} \left[ \beta^{\text{dyn}} \mathcal{L}_t^{\text{dyn}}(\phi) + \beta^{\text{rep}} \mathcal{L}_t^{\text{rep}}(\phi) + \mathcal{L}_t^{\text{rew}}(\phi) + \mathcal{L}_t^{\text{con}}(\phi) \right]$$

where  $\beta^{\text{dyn}}$  and  $\beta^{\text{rep}}$  are the weight factors.

#### D. Agent

1) *Learning Algorithm:* We adopt an actor-critic structure inspired by DreamerV3 to develop the driving policy [6]. The agent's input state  $s_t$  is composed of a concatenation of the latent feature  $z_t$  and the hidden state  $h_t$ . The agent's action  $a_t$  is sampled from the policy  $\pi_\theta(a_t|s_t)$  held in the actor network, where  $\theta$  represents the parameters of the actor network.

$$\begin{aligned}\text{State:} & \quad s_t = [z_t, h_t] \\ \text{Action:} & \quad a_t \sim \pi_\theta(a_t|s_t)\end{aligned}$$

The critic network evaluates the policy's performance by the state-value function  $V_\varphi(s_t)$ .

$$V_\varphi(s_t) \triangleq \mathbb{E}_{\pi_\theta} \left[ \sum_{k=1}^{\infty} \gamma^{k-1} r_{t+k} | s_t \right]$$

where  $\varphi$  represents the parameters of the critic network and  $\gamma$  is the discount factor for future rewards.

Similar to DreamerV3, we employ the  $\lambda$ -return  $G_t^\lambda$  to balance short-term and long-term rewards effectively.

$$G_t^\lambda = r_{t+1} + c_t \cdot \gamma \left[ (1 - \lambda)V(s_{t+1}) + \lambda G_{t+1}^\lambda \right]$$

The variable  $c_t$  describes whether the episode continues at time  $t$ . Obviously, if the episode ends, the future return should be reset to zero.

The loss of the actor and the critic networks are described as follows:

$$\begin{aligned}\mathcal{L}(\theta) &= \mathbb{E} \left[ -\text{sg} \left( \frac{G_t^\lambda - V_\varphi(s_t)}{\max(1, S)} \right) - \eta H(\pi_\theta(a_t|s_t)) \right] \\ \mathcal{L}(\varphi) &= \mathbb{E} \left[ (V_\varphi(s_t) - \text{sg}(G_t^\lambda))^2 + (V_\varphi(s_t) - \text{sg}(V_{\varphi\text{EMA}}(s_t)))^2 \right]\end{aligned}$$

where  $H(\cdot)$  is the entropy function and  $\eta$  is the coefficient for entropy loss.  $S$  in actor's loss is a normalization ratio:

$$S = \text{percentile}(G_t^\lambda, 95) - \text{percentile}(G_t^\lambda, 5)$$

Originally, the critic's loss included only the first term. STORM recommends incorporating the exponential moving average (EMA) of the critic network to stabilize the training process and reduce the risk of overfitting.

#### 2) Reward Function:

$$\begin{aligned}r_t^{\text{col}} &= \begin{cases} -2, & \text{collided with other pedestrian} \\ -1.8, & \text{collided with other vehicle} \\ -1.6, & \text{collided with other object} \\ 0, & \text{no collision} \end{cases} \\ r_t^{\text{vio}} &= \begin{cases} -1.4, & \text{violated stop sign} \\ -1.2, & \text{violated other rules} \\ 0, & \text{no violation} \end{cases} \\ r_t^{\text{con}} &= \begin{cases} 0.1, & \text{continuing the route} \\ 0, & \text{interrupted} \end{cases} \\ r_t^{\text{spe}} &= \tanh(v_t - v_{\min}) + 1 \\ r_t^{\text{rou}} &= \mathcal{RC}_t - \mathcal{RC}_{t-1} \\ r_t &= r_t^{\text{col}} + r_t^{\text{vio}} + r_t^{\text{con}} + r_t^{\text{spe}} + r_t^{\text{rou}}\end{aligned}$$

#### E. Training Recipe

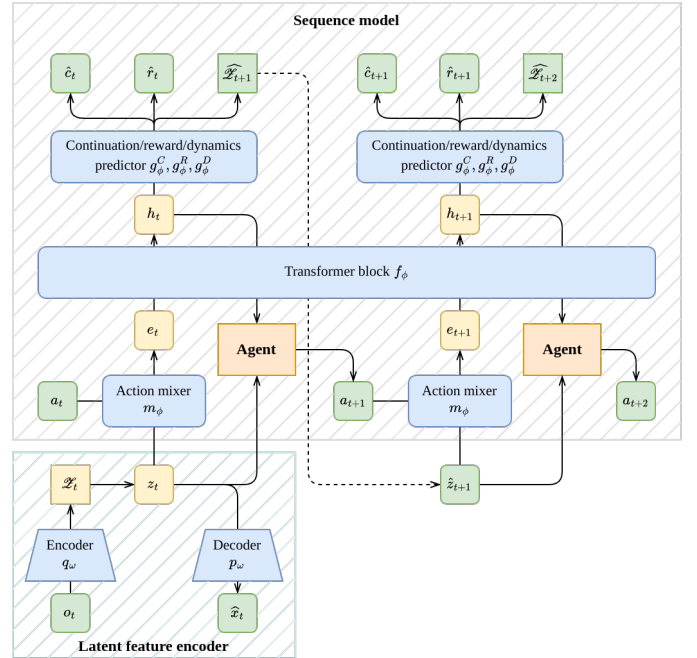


Fig. 3. Ramble infers the actions from  $t$  to  $t+n$ . The actions since  $t+1$  are generated based on imagination.

## IV. EXPERIMENT

### A. Benchmarks

We evaluated our methods using CARLA's official benchmarks: Leaderboard 1.0 and Leaderboard 2.0. Leaderboard 1.0 provides routes without any special events in relatively small maps, while Leaderboard 2.0 adds 39 types of challenging interactive traffic scenarios to the routes in large maps. These benchmarks facilitate a relatively fair comparison of different methods by offering an online platform where users can test their methods on unseen route sets. We selected Leaderboard 1.0 because it is the most widely acknowledged benchmark for comparing end-to-end driving methods [9]. Meanwhile,

Leaderboard 2.0 is appealing because of the more rigorous test, which better exposes the limitations of current state-of-the-art methods evaluated under Leaderboard 1.0.

### B. Evaluation Metrics

The CARLA Leaderboards employ three key metrics to assess model performance: route completion, infraction penalty, and driving score. Route completion measures the average ratio of successfully completed routes. Infraction penalty reflects adherence to traffic regulations, diminishing by a percentage when the agent commits infractions or violates traffic rules. The driving score is derived from the product of the route completion ratio and infraction penalty. It offers a comprehensive evaluation of the agent’s efficiency and safety. The detailed infraction items are defined and automatically obtained by the CARLA leaderboards, including

- collision with pedestrians (*Collisions pedestrians*)
- collision with other vehicles (*Collisions vehicles*)
- collision with static elements (*Collisions layout*)
- running a *Red light*
- running a *Stop sign*
- driving *Off-road*
- agent taking no action for a long time (*Agent blocked*)
- failure to *Yield to emergency* vehicle
- failure to maintain *Minimum speed*
- failure to pass a scenario in time (*Scenario timeouts*) - This metric is only available in Leaderboard 2.0 because “scenario” is defined before.
- deviation from the routes for a distance (*Route deviations*)
- failure to complete a route in time (*Route timeout*)

### C. Experts

Due to the difficulty of the routes in CARLA’s leaderboards, most end-to-end driving models cannot guarantee the completion of all the routes without relying on privileged information, such as the ground-truth states of surrounding traffic participants, precise positions of static obstacles, and the specific details of traffic signs. To estimate the upper limit performance of learning-based end-to-end driving models, we adapted several representative experts.

1) *Roach*: The RL-based expert developed by [3] serves as the coach that guides the training of the IL agent using only permissible data. This model leverages the states of traffic lights and semantic segmentation images as privileged information, effectively demonstrating RL’s capability to formulate driving policies from scratch. We reproduced the performance of Roach’s expert model on CARLA Leaderboard 1.0, and then adapted and trained it on CARLA Leaderboard 2.0. This approach allows us to illustrate the potential upper limits of model-free RL’s performance in autonomous driving scenarios.

2) *Think2Drive*: Think2Drive is an RL-based expert model incorporating a world model to enhance its understanding of the environment [4]. It stands out as the first learning-based model to successfully complete routes on CARLA Leaderboard 2.0. Still, it relies on some privileged information, including real-time bounding boxes of surrounding traffic participants and obstacles, HD maps, and the states of traffic

lights. Due to the code’s unavailability<sup>1</sup> and the substantial computational resources required, we reference the scores reported in Think2Drive’s publication to illustrate the potential performance of learning-based models.

3) *PDM-Lite*: PDM-Lite is a rule-based expert model developed by [1] to gather data from CARLA Leaderboard 2.0. It is the only open-source model reported to achieve a 100% route completion rate on most of the routes in Leaderboard 2.0. This model extracts scenario types and traffic signals from the backend, generating a list of feasible waypoints. It employs bicycle models to predict trajectories for both the ego vehicle and nearby traffic participants. Using the gathered contexts, it calculates control commands through a longitudinal linear regression controller and a lateral PID controller. Due to its heavy reliance on identifying scenario types, an attribute absent in Leaderboard 1.0, PDM-Lite is only referred to for performance comparison in Leaderboard 2.0.

### D. Baselines

We have reproduced various SOTA driving models on CARLA Leaderboard 1.0 and transited them to Leaderboard 2.0 to assess their ability of generalization. Notably, all the end-to-end driving models achieving top positions on the leaderboards are based on IL. IL possesses an advantage over model-free RL in its superior capacity to handle high-dimensional environmental data. Additionally, the availability of ground truth trajectory data facilitates faster convergence in the policy network. The absence of standout RL-based state-of-the-art models is another reason why we introduce RL-based expert models for comparison experiments.

1) *LAV*: LAV processes multi-modal sensory data, including RGB camera and LiDAR inputs, to directly output control commands [18]. The model is elegantly designed, emphasizing that the quality of the ground truth trajectory during training significantly influences performance. This model was selected because it ranks 1st regarding route completion rate on CARLA Leaderboard 1.0.

2) *Transfuser++*: Transfuser++ is an enhanced version of Transfuser [11, 15], maintaining a similar structure while improving the transformer’s efficiency and reducing ambiguity in the model’s output by disentangling trajectory prediction from velocity. Among the various implementations of Transfuser++, we opted to reproduce the version with waypoint prediction (TF++ WP) and adapted it for CARLA Leaderboard 2.0.

3) *TCP*: TCP is a camera-only IL model [14], which proposes combining trajectory and control prediction outputs to enhance the model’s generalization ability. This innovative framework allows TCP to be seamlessly integrated as an output module for other models. We have reproduced TCP’s performance on CARLA Leaderboard 1.0 and transited it to Leaderboard 2.0 to evaluate its generalization ability.

4) *ReasonNet*: ReasonNet is the successor to InterFuser [12, 13]. Its main improvement is the introduction of a global reasoning module that enhances the model’s environmental understanding. This model has achieved the highest driving

<sup>1</sup>Li and Jia’s lab is located upstairs from us. We have checked with them that they have no plan to open-source their code recently.

TABLE I  
PERFORMANCE COMPARISON IN CARLA LEADERBOARD 1.0. THE METHODS MARKED WITH \* ARE NOT REPRODUCED BY US.

Method	DS	RC	IS	Collisions pedestrians	Collisions vehicles	Collisions layout	Red light	Stop sign	Off-road	Agent blocked	Route deviations	Route timeout
	%, ↑	%, ↑	↑	#/km, ↓	#/km, ↓	#/km, ↓	#/km, ↓	#/km, ↓	#/km, ↓	#/km, ↓	#/km, ↓	#/km, ↓
Roach [3]	78.1	98.6	0.80	0.00	0.30	0.00	0.05	0.03	0.00	0.06	0.00	0.05
Think2Drive* [4]	90.2	99.7	-	-	-	-	-	-	-	-	-	-
ReasonNet* [13]	80.0	89.9	0.89	0.02	0.13	0.01	0.08	0.00	0.04	0.33	0.00	0.01
LAV [18]	61.85	94.46	0.64	0.04	0.70	0.02	0.17	0.00	0.25	0.10	0.09	0.04
TF++ [15]	66.32	78.57	0.84	0.00	0.50	0.00	0.01	0.00	0.12	0.71	0.00	0.00
TCP [14]	75.14	85.63	0.87	0.00	0.32	0.00	0.09	0.00	0.04	0.54	0.00	0.00
Ramble (Ours)												

TABLE II  
PERFORMANCE COMPARISON IN CARLA LEADERBOARD 2.0. THE METHODS MARKED WITH \* ARE NOT REPRODUCED BY US.

Method	DS	RC	IS	Collisions pedestrians	Collisions vehicles	Collisions layout	Red light	Stop sign	Off-road	Agent blocked	Yield emergency	Min speed	Scenario timeouts	Route deviations	Route timeout
	%, ↑	%, ↑	↑	#/km, ↓	#/km, ↓	#/km, ↓	#/km, ↓	#/km, ↓	#/km, ↓	#/km, ↓	#/km, ↓	#/km, ↓	#/km, ↓	#/km, ↓	#/km, ↓
Roach [3]															
Think2Drive* [4]	56.8	98.6	-	-	-	-	-	-	-	-	-	-	-	-	-
PDM-Lite [1]	43.6	96.4	0.45	0.00	0.10	0.07	0.00	0.00	0.00	0.00	0.02	0.02	0.06	0.00	0.00
CarLLaVA* [1]	6.9	18.1	0.42	0.05	1.17	0.05	0.00	0.11	0.01	0.45	0.00	0.00	0.13	0.08	0.00
LAV [18]															
TF++ [15]															
TCP [14]															
Ramble (Ours)															

score on the CARLA Leaderboard 1.0. However, the code for ReasonNet has not been made public. Given that reproductions of InterFuser have shown a significant drop in performance<sup>2</sup>, we cannot ensure the reproduction of ReasonNet would achieve similar results. Consequently, our comparison in Table I is based on the scores reported in the leaderboard.

5) *CarLLaVA*: CarLLaVA is an IL-based driving model that leverages a large language model LLaMA to encode the environmental context and imitate driving behavior generated by PDM-Lite [1]. This model has achieved the highest driving score on the CARLA Leaderboard 2.0. The code for CarLLaVA has not been made public. Moreover, we cannot afford to train a model with the same scale as CarLLaVA due to a limit in computational resources. Therefore, our comparison in Table II is based on the scores reported in the leaderboard.

### E. Devices

When developing our model, we utilized a server equipped with four GeForce RTX 3090 GPUs to implement our method and obtain trained results. However, due to resource limitations, we conducted our efficiency comparison experiments on a server outfitted with a single i9-10920X CPU (24 cores) and two GeForce RTX 3090 GPUs.

## V. RESULT AND DISCUSSION

### A. Comparison of Performance

In Tables I and II, we present a performance comparison between the baseline methods and our proposed approaches,

based on the evaluation metrics defined by CARLA (as detailed in Section IV-B).

Table I presents the results on CARLA Leaderboard 1.0. For expert models that utilize privileged information, we report offline test results based on the testing routes provided by the official leaderboard. The other algorithms were submitted to the online leaderboard for a more rigorous evaluation.

Table II shows the results on CARLA Leaderboard 2.0. Offline test results are provided for expert models using privileged information, based on the official validation routes. Due to recurring crashes in the CARLA simulator when running routes 3 and 13, we excluded these routes from our tests. The remaining algorithms were evaluated via the online leaderboard to ensure a more convincing assessment.

The algorithms marked with a star indicate those for which we were unable to reproduce the results due to limited access to source code and large-scale computational resources. For these cases (Think2Drive, ReasonNet, and CarLLaVA), we directly reference the results reported in the original papers.

Roach follows the implementation of ThinkTwice [38], which version reaches a higher driving score than the original.

### B. Comparison of Efficiency

<sup>2</sup>See <https://paperswithcode.com/sota/autonomous-driving-on-carla-leaderboard>. Table III and IV

TABLE III  
EFFICIENCY COMPARISON IN CARLA LEADERBOARD 1.0

Method	Training				Running			
	Episodes #	Time per episode minutes	Memory GB, ↓	GPU GB, ↓	Average step duration ms, ↓	Average speed m/s, ↑	Memory GB, ↓	GPU GB, ↓
Roach [3]								
LAV [18] TF++ WP [15] TCP [14]								
Ramble (Ours)								

TABLE IV  
EFFICIENCY COMPARISON IN CARLA LEADERBOARD 2.0

Method	Training				Running			
	Episodes #	Time per episode minutes	Memory GB, ↓	GPU GB, ↓	Average step duration ms, ↓	Average speed m/s, ↑	Memory GB, ↓	GPU GB, ↓
Roach [3] PDM-Lite [1]	-	-	-	-			10	0
LAV [18] TF++ WP [15] TCP [14]								
Ramble (Ours)								

### C. Ablation Study

### D. Visualization

## VI. CONCLUSION

### REFERENCES

- [1] K. Renz, L. Chen, A.-M. Marcu, J. Hünermann, B. Hanotte, A. Karnsund, J. Shotton, E. Arani, and O. Sinavski, “Carllava: Vision language models for camera-only closed-loop driving,” *arXiv preprint arXiv:2406.10165*, 2024.
- [2] P. R. Wurman, S. Barrett, K. Kawamoto, J. MacGlashan, K. Subramanian, T. J. Walsh, R. Capobianco, A. Devlic, F. Eckert, F. Fuchs *et al.*, “Outracing champion gran turismo drivers with deep reinforcement learning,” *Nature*, vol. 602, no. 7896, pp. 223–228, 2022.
- [3] Z. Zhang, A. Liniger, D. Dai, F. Yu, and L. Van Gool, “End-to-end urban driving by imitating a reinforcement learning coach,” in *Proceedings of the IEEE/CVF international conference on computer vision*, 2021, pp. 15 222–15 232.
- [4] Q. Li, X. Jia, S. Wang, and J. Yan, “Think2drive: Efficient reinforcement learning by thinking in latent world model for quasi-realistic autonomous driving (in carla-v2),” *arXiv preprint arXiv:2402.16720*, 2024.
- [5] K. Arulkumaran, M. P. Deisenroth, M. Brundage, and A. A. Bharath, “Deep reinforcement learning: A brief survey,” *IEEE Signal Processing Magazine*, vol. 34, no. 6, pp. 26–38, 2017.
- [6] D. Hafner, J. Pasukonis, J. Ba, and T. Lillicrap, “Mastering diverse domains through world models,” *arXiv preprint arXiv:2301.04104*, 2023.
- [7] B. R. Kiran, I. Sobh, V. Talpaert, P. Mannion, A. A. Al Sallab, S. Yogamani, and P. Pérez, “Deep reinforcement learning for autonomous driving: A survey,” *IEEE Transactions on Intelligent Transportation Systems*, vol. 23, no. 6, pp. 4909–4926, 2021.
- [8] S. Lu, L. He, S. E. Li, Y. Luo, J. Wang, and K. Li, “Hierarchical end-to-end autonomous driving: Integrating bev perception with deep reinforcement learning,” *arXiv preprint arXiv:2409.17659*, 2024.
- [9] P. S. Chib and P. Singh, “Recent advancements in end-to-end autonomous driving using deep learning: A survey,” *IEEE Transactions on Intelligent Vehicles*, vol. 9, no. 1, pp. 103–118, 2024.
- [10] M. Bojarski, D. Del Testa, D. Dworakowski, B. Firner, B. Flepp, P. Goyal, L. D. Jackel, M. Monfort, U. Muller, J. Zhang *et al.*, “End to end learning for self-driving cars,” *arXiv preprint arXiv:1604.07316*, 2016.
- [11] K. Chitta, A. Prakash, B. Jaeger, Z. Yu, K. Renz, and A. Geiger, “Transfuser: Imitation with transformer-based sensor fusion for autonomous driving,” *IEEE Transactions on Pattern Analysis and Machine Intelligence*, 2022.
- [12] H. Shao, L. Wang, R. Chen, H. Li, and Y. Liu, “Safety-enhanced autonomous driving using interpretable sensor fusion transformer,” in *Conference on Robot Learning*. PMLR, 2023, pp. 726–737.
- [13] H. Shao, L. Wang, R. Chen, S. L. Waslander, H. Li, and Y. Liu, “Reasonnet: End-to-end driving with temporal and global reasoning,” in *Proceedings of the IEEE/CVF Conference on Computer Vision and Pattern Recognition*, 2023, pp. 13 723–13 733.
- [14] P. Wu, X. Jia, L. Chen, J. Yan, H. Li, and Y. Qiao,



- “Trajectory-guided control prediction for end-to-end autonomous driving: A simple yet strong baseline,” *Advances in Neural Information Processing Systems*, vol. 35, pp. 6119–6132, 2022.
- [15] B. Jaeger, K. Chitta, and A. Geiger, “Hidden biases of end-to-end driving models,” in *Proceedings of the IEEE/CVF International Conference on Computer Vision*, 2023, pp. 8240–8249.
- [16] H. Xu, Y. Gao, F. Yu, and T. Darrell, “End-to-end learning of driving models from large-scale video datasets,” in *Proceedings of the IEEE conference on computer vision and pattern recognition*, 2017, pp. 2174–2182.
- [17] D. Chen, B. Zhou, V. Koltun, and P. Krähenbühl, “Learning by cheating,” in *Conference on Robot Learning*, PMLR, 2020, pp. 66–75.
- [18] D. Chen and P. Krähenbühl, “Learning from all vehicles,” in *Proceedings of the IEEE/CVF Conference on Computer Vision and Pattern Recognition*, 2022, pp. 17 222–17 231.
- [19] A. E. Sallab, M. Abdou, E. Perot, and S. Yogamani, “End-to-end deep reinforcement learning for lane keeping assist,” *arXiv preprint arXiv:1612.04340*, 2016.
- [20] P. Zhang, L. Xiong, Z. Yu, P. Fang, S. Yan, J. Yao, and Y. Zhou, “Reinforcement learning-based end-to-end parking for automatic parking system,” *Sensors*, vol. 19, no. 18, p. 3996, 2019.
- [21] A. Kendall, J. Hawke, D. Janz, P. Mazur, D. Reda, J.-M. Allen, V.-D. Lam, A. Bewley, and A. Shah, “Learning to drive in a day,” in *2019 international conference on robotics and automation (ICRA)*. IEEE, 2019, pp. 8248–8254.
- [22] M. Toromanoff, E. Wirbel, and F. Moutarde, “End-to-end model-free reinforcement learning for urban driving using implicit affordances,” in *Proceedings of the IEEE/CVF conference on computer vision and pattern recognition*, 2020, pp. 7153–7162.
- [23] Y. Zhao, K. Wu, Z. Xu, Z. Che, Q. Lu, J. Tang, and C. H. Liu, “Cadre: A cascade deep reinforcement learning framework for vision-based autonomous urban driving,” in *Proceedings of the AAAI conference on artificial intelligence*, vol. 36, no. 3, 2022, pp. 3481–3489.
- [24] Z. M. Peng, W. Mo, C. Duan, Q. Li, and B. Zhou, “Learning from active human involvement through proxy value propagation,” *Advances in neural information processing systems*, vol. 36, 2024.
- [25] T. M. Moerland, J. Broekens, A. Plaat, C. M. Jonker *et al.*, “Model-based reinforcement learning: A survey,” *Foundations and Trends® in Machine Learning*, vol. 16, no. 1, pp. 1–118, 2023.
- [26] D. Ha and J. Schmidhuber, “World models,” *arXiv preprint arXiv:1803.10122*, 2018.
- [27] L. Kaiser, M. Babaeizadeh, P. Milos, B. Osinski, R. H. Campbell, K. Czechowski, D. Erhan, C. Finn, P. Kozakowski, S. Levine *et al.*, “Model-based reinforcement learning for atari,” *arXiv preprint arXiv:1903.00374*, 2019.
- [28] D. Hafner, T. Lillicrap, I. Fischer, R. Villegas, D. Ha, H. Lee, and J. Davidson, “Learning latent dynamics for planning from pixels,” in *International conference on machine learning*. PMLR, 2019, pp. 2555–2565.
- [29] W. Ye, S. Liu, T. Kurutach, P. Abbeel, and Y. Gao, “Mastering atari games with limited data,” *Advances in neural information processing systems*, vol. 34, pp. 25 476–25 488, 2021.
- [30] W. Zhang, G. Wang, J. Sun, Y. Yuan, and G. Huang, “Storm: Efficient stochastic transformer based world models for reinforcement learning,” *Advances in Neural Information Processing Systems*, vol. 36, 2024.
- [31] M. G. Bellemare, Y. Naddaf, J. Veness, and M. Bowling, “The arcade learning environment: An evaluation platform for general agents,” *Journal of Artificial Intelligence Research*, vol. 47, pp. 253–279, 2013.
- [32] T. Liang, H. Xie, K. Yu, Z. Xia, Z. Lin, Y. Wang, T. Tang, B. Wang, and Z. Tang, “Bevfusion: A simple and robust lidar-camera fusion framework,” *Advances in Neural Information Processing Systems*, vol. 35, pp. 10 421–10 434, 2022.
- [33] Z. Liu, Y. Lin, Y. Cao, H. Hu, Y. Wei, Z. Zhang, S. Lin, and B. Guo, “Swin transformer: Hierarchical vision transformer using shifted windows,” in *Proceedings of the IEEE/CVF international conference on computer vision*, 2021, pp. 10 012–10 022.
- [34] T.-Y. Lin, P. Dollár, R. Girshick, K. He, B. Hariharan, and S. Belongie, “Feature pyramid networks for object detection,” in *Proceedings of the IEEE conference on computer vision and pattern recognition*, 2017, pp. 2117–2125.
- [35] A. H. Lang, S. Vora, H. Caesar, L. Zhou, J. Yang, and O. Beijbom, “Pointpillars: Fast encoders for object detection from point clouds,” in *Proceedings of the IEEE/CVF conference on computer vision and pattern recognition*, 2019, pp. 12 697–12 705.
- [36] V. Micheli, E. Alonso, and F. Fleuret, “Transformers are sample-efficient world models,” *arXiv preprint arXiv:2209.00588*, 2022.
- [37] T.-Y. Lin, P. Goyal, R. Girshick, K. He, and P. Dollár, “Focal loss for dense object detection,” in *Proceedings of the IEEE international conference on computer vision*, 2017, pp. 2980–2988.
- [38] X. Jia, P. Wu, L. Chen, J. Xie, C. He, J. Yan, and H. Li, “Think twice before driving: Towards scalable decoders for end-to-end autonomous driving,” in *Proceedings of the IEEE/CVF Conference on Computer Vision and Pattern Recognition*, 2023, pp. 21 983–21 994.



**Yueyuan LI** received a Bachelor’s degree in Electrical and Computer Engineering from the University of Michigan-Shanghai Jiao Tong University Joint Institute, Shanghai, China in 2020. She is pursuing a Ph.D. degree in Control Science and Engineering from Shanghai Jiao Tong University.

Her main fields of interest are the security of the autonomous driving system and driving decision-making. Her current research activities include driving decision-making models, driving simulation, and virtual-to-real model transferring.



**Mingyang Jiang** received a Bachelor's degree in engineering from Shanghai Jiao Tong University, Shanghai, China, in 2023. He is working towards a Master's degree in Control Science and Engineering from Shanghai Jiao Tong University. His main research interests are end-to-end planning, driving decision-making, and reinforcement learning for autonomous vehicles.



**Songan Zhang** received B.S. and M.S. degrees in automotive engineering from Tsinghua University in 2013 and 2016, respectively. Then, she went to the University of Michigan, Ann Arbor, and got a Ph.D. in mechanical engineering in 2021. After graduation, she worked as a research scientist on the Robotics Research Team at Ford Motor Company. Presently, she is an assistant professor at the Global Institute of Future Technology (GIFT) at Shanghai Jiao Tong University. Her research interests include accelerated evaluation of autonomous vehicles, model-based re-

inforcement learning, and meta-reinforcement learning for autonomous vehicle decision-making.



**Wei YUAN** received his Master's and Ph.D. degrees in Automation from Shanghai Jiao Tong University, Shanghai, China, in 2017 and 2021, respectively. Presently, he is a postdoctoral researcher at Shanghai Jiao Tong University.

His main fields of interest are autonomous driving systems, computer vision, deep learning, and vehicle control. His current research activities include end-to-end learning-based vehicle control and decision-making.



**Chunxiang WANG** received a Ph.D. degree in Mechanical Engineering from Harbin Institute of Technology, China, in 1999. She is currently an associate professor in the Department of Automation at Shanghai Jiao Tong University, Shanghai, China.

She has been working in the field of intelligent vehicles for more than ten years and has participated in several related research projects, such as European CyberC3 project, ITER transfer cask project, etc. Her research interests include autonomous driving, assistant driving, and mobile robots.



**Ming YANG** received his Master's and Ph.D. degrees from Tsinghua University, Beijing, China, in 1999 and 2003, respectively. Presently, he holds the position of Distinguished Professor at Shanghai Jiao Tong University, also serving as the Director of the Innovation Center of Intelligent Connected Vehicles. Dr. Yang has been engaged in the research of intelligent vehicles for more than 25 years.

APPENDIX A  
DETAILS OF MODEL STRUCTURE

TABLE V

<b>Annotation</b>	<b>Description</b>
$t$	Time
$o_t$	Raw sensor inputs at time $t$
$x_t$	The ground truth semantic segmentation at time $t$
$\hat{x}_t$	The estimated semantic segmentation at time $t$
$a_t$	The action taken at time $t$

APPENDIX B  
SENSOR CONFIGURATION

TABLE VI  
CAPTION

<b>Sensor</b>	x	y	z	roll	pitch	yaw	FOV
Camera (front)	0.2	0.0	1.8	0°	0°	0°	120°
Camera (left)	-0.1	-0.4	1.8	0°	-15°	-90°	120°
Camera (right)	-0.1	0.4	1.8	0°	-15°	90°	120°
Camera (rear)	-0.5	0.0	1.8	0°	0°	180°	120°
LiDAR	0.0	0.0	2.0	0°	0°	0°	360°
IMU	0.0	0.0	0.0	0°	0°	0°	-
GPS	0.0	0.0	0.0	0°	0°	0°	-